J|A|C|S
COMMUNICATIONS

Published on Web 03/11/2004

Fast Lithium Ion Diffusion in the Ternary Layered Nitridometalate LiNiN

Zlatka Stoeva,[†] Ruben Gomez,[†] Alexandra G. Gordon,[†] Mark Allan,[†] Duncan H. Gregory,*[,†] Gary B. Hix,[‡] and Jeremy J. Titman[†]

School of Chemistry, University of Nottingham, University Park, Nottingham, NG7 2RD, U.K., and School of Molecular Sciences, The Hawthorn Building, De Montfort University, The Gateway, Leicester, LE1 9BH, U.K.

Received November 14, 2003; E-mail: duncan.gregory@nottingham.ac.uk

Lithium late transition-metal nitrides, originally described as $Li_{3-x}M_xN$ (M = Cu, Ni, Co), are isostructural with Li_3N and exhibit hexagonal layered structures with alternating $[Li_2N]$ and Li/M planes.[1] The introduction of a transition metal has important implications for the electronic, conduction, and magnetic properties. Recently, Li_3N-derived ternary nitrides have aroused interest as possible anode materials in lithium secondary batteries.[2−6] However, at the microscopic level, the electrochemistry and dynamics in lithium nitridometalates are poorly understood.

Our recent structural investigations of the Li−Ni−N system reveal ordered and disordered phases with significant levels of lithium vacancies: $Li_{3-x-y}Ni_xN$ (y = vacancy).[7,8] Li vacancies are the charge carriers in Li_3N, itself a well-known fast ion conductor with the highest Li^+ conductivity observed in a crystalline solid electrolyte at ambient temperature.[9,10] The formation of additional vacancies in the ternary phases implies a potential for enhanced lithium ion diffusion.

Disordered phases $Li_{3-x-y}Ni_xN$ are formed for $x = 0-0.8$.[8,11,12] Their structures are defect Li_3N-type where the transition metal partially and aliovalently replaces interlayer lithium, Li(1). Ensuing lithium vacancies are randomly distributed within $[Li_{2-y}N]$ planes. In the ordered phases $Li_5Ni_3N_3$ and LiNiN ($x = 1$), interlayer lithium is completely replaced, and vacancies are ordered within the $[Li_{2-y}N]$ planes.[7] Vacancy ordering is concomitant with a structure transition (from $P6/mmm$ in Li_3N to $P\bar{6}m2$ in LiNiN or $P\bar{6}2m$ in $Li_5Ni_3N_3$). Disordered phases can be obtained by heating stoichiometric mixtures of Li_3N and Ni powders.[1] The preparation of ordered phases requires carefully controlled conditions.[13]

Single-crystal X-ray diffraction studies suggest that LiNiN has the highest concentration of vacancies in the Li−Ni−N system.[7] Within LiNiN, alternate $[LiN]^{2-}$ planes and Ni^{2+} ions stack perpendicular to the c-axis[7,14] (Figure 1). The [LiN] planes are linked via infinite, perpendicular N−Ni−N chains, $^1_\infty[NiN_{2/2}]$. Nitrogen is five-coordinate (to three Li and two Ni), thus forming trigonal bipyramids linked by vertexes in three dimensions. The lithium coordination in the [LiN] planes is trigonal planar, as in the parent compound Li_3N. In this communication, we describe studies of the local structure and dynamics using ^{7}Li solid-state NMR and of magnetic properties by SQUID magnetometry.

^{7}Li NMR spectra (Figure 2) were recorded between 120 and 473 K using powder samples of LiNiN and the parent Li_3N at 77.7 MHz with a variable-temperature static NMR probe.[15] The parent Li_3N shows motional narrowing between 180 and 290 K, which was ascribed previously[16] to the onset of Li^+ intralayer diffusion. Above 290 K, the Li_3N satellites broaden again, due to Li^+ interlayer diffusion via exchange between Li(1) and Li(2) sites.[16] For LiNiN, the spectra vary with temperature in a fashion similar to the "universal" behavior observed previously[17] for LISICON and phosphate lithium superionic conductors. At low temperatures, the quadrupolar satellites are broadened and lost in the baseline. Above 200 K, motional narrowing occurs (Figure 3a, □) due to Li^+ diffusion, while at 280 K, well-resolved satellites with a reduced quadrupolar coupling constant begin to appear. This indicates that the Li^+ diffusion occurs only within the [LiN] planes in LiNiN. A straightforward measurement of the central transition dipolar line

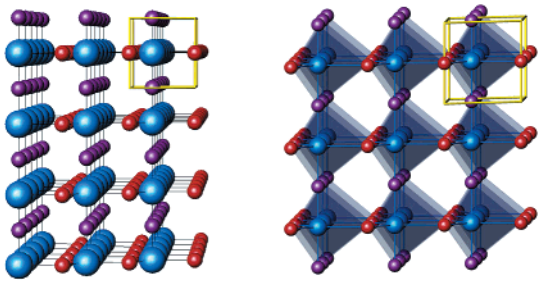

Figure 1. Structure of LiNiN (space group $P\bar{6}m2$), with the unit cell outlined. N atoms are drawn as blue spheres, Li atoms as red spheres, and Ni atoms as purple spheres. The blue polyhedra show the trigonal bipyramidal coordination of nitrogen atoms.

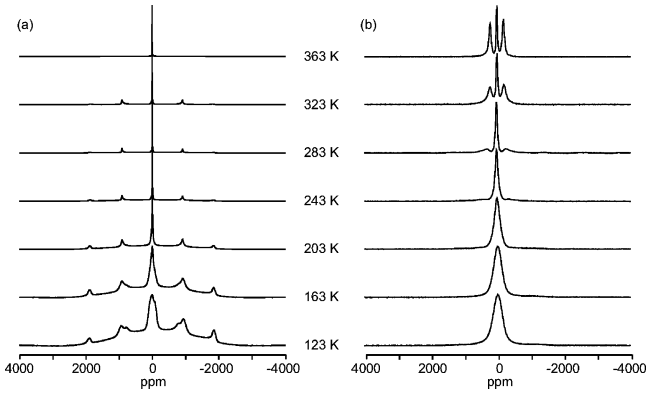

Figure 2. ^{7}Li NMR spectra of (a) Li_3N and (b) LiNiN recorded as a function of temperature as described in the text.

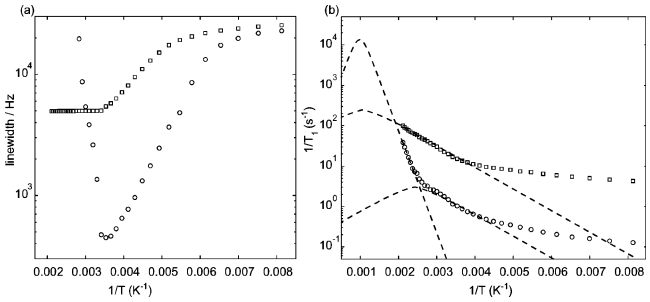

Figure 3. (a) ^{7}Li NMR line widths and (b) T_1 relaxation times recorded as described in the text for Li_3N (Li(2) satellites, ○) and LiNiN (central transition, □).

[†] University of Nottingham.
[‡] De Montfort University.

10.1021/ja039603b CCC: $27.50

Table 1. Li^+ Intralayer Diffusion Parameters from NMR Data

	Li_3N		LiNiN	
	line width	T_1	line width	T_1
E_a/eV	0.121	0.122	0.068	0.066
τ(298 K)/(10^{-7} s)	2.77	2.83	35.2	32.2
D(298 K)/(10^{-14} m^2 s^{-1})	9.02	8.84	0.638	0.697

width (Figure 3a, ○) is possible in LiNiN where only the Li(2) site is present. Hence, following the analysis in ref 16, the mean Li^+ jump rate ($1/\tau$), the diffusion coefficient (D), and the activation energy (E_a) for Li^+ intralayer diffusion in LiNiN were obtained. These are given in Table 1, along with the corresponding quantities for Li_3N, which are comparable with those given in ref 16. As in previous work,[16] the overlap of the central transitions for the Li(1) and Li(2) sites in Li_3N necessitates the measurement of the Li(2) satellite line widths. From Table 1, the E_a for LiNiN is reduced compared to Li_3N, and $1/\tau$ and D at 298 K are lower. The reduction in the Li^+ jump rate may arise from the entropic effects of vacancy ordering in LiNiN. However, despite the structural differences between Li_3N and LiNiN, the Li^+ intralayer diffusion is very similar.

^{7}Li spin−lattice relaxation time (T_1) measurements on Li_3N and LiNiN confirmed the conclusions of the line width studies. For Li_3N,[18,19] there are two relaxation regimes due to interlayer and intralayer diffusion at high and low temperatures, respectively (Figure 3b, ○). At 77.7 MHz, the T_1 minimum for the high temperature relaxation process occurs above the maximum temperature of 473 K available with our apparatus. For LiNiN, only a single relaxation regime is observed (Figure 3b, □), confirming that diffusion is limited to one of the two mechanisms present in Li_3N. A simple BPP analysis[18] yields diffusion parameters for Li^+ intralayer diffusion (Table 1), which are in good agreement with those obtained from the line width measurements. Without the T_1 minimum, a more detailed analysis[17,19] was not attempted.

Magnetic susceptibility measurements[20] show that Li_3N exhibits very weak temperature-independent paramagnetism in the range 5−250 K. In the same temperature range, the magnetic susceptibility of LiNiN is higher, but of the same order of magnitude and almost independent of temperature. This type of magnetic behavior is characteristic of itinerant spin systems and suggests that LiNiN could be metallic.[21] This premise is not unreasonable given the structure and the band structure of the semiconducting parent, Li_3N.[22] Although the origin of the metallic properties of LiNiN is not yet known, the straight $^1_\infty[NiN_{2/2}]$ chains in the structure could be expected to lead to low-dimensional electronic and magnetic behavior. The small Curie−Weiss contribution to the magnetism in LiNiN probably arises from local defects in the $^1_\infty[NiN_{2/2}]$ chains where Li atoms occupy interplanar (Ni) sites. Similar magnetism is observed in metallic CaNiN, also containing straight $^1_\infty[NiN_{2/2}]$ chains.[23]

The ^{7}Li shift (30 ppm relative to 1 M LiCl (aq)) in LiNiN[24] is almost independent of temperature, indicative of Pauli paramagnetism.[25] In contrast, larger (up to 2000 ppm) temperature-dependent ^{6}Li and ^{7}Li NMR shifts are observed in Li−Mn−O spinels where the NMR behavior is dominated by Curie−Weiss paramagnetism.[26]

In conclusion, we have demonstrated that layered LiNiN exhibits significant Li^+ diffusion, likely combined with electronic conductivity. ^{7}Li NMR relaxation measurements suggest that Li^+ diffusion takes place via an intralayer process only. E_a in the ternary material is reduced, commensurate with a weakening (lengthening) of the Li−N intralayer bond. These properties make LiNiN attractive for further experimental and theoretical investigation and a strong candidate as an anode material. We are currently examining the transport, electrochemical, and magnetic properties of LiNiN in more detail.

Acknowledgment. This research was carried out under EPSRC Grant GR/R87345. R.G. thanks Resonance Instruments (Witney, U.K.) for financial support.

Supporting Information Available: Powder X-ray diffraction data for LiNiN and SQUID data for Li_3N and LiNiN (TIF). This material is available free of charge via the Internet at http://pubs.acs.org.

References

(1) Sachsze, W.; Juza, R. *Z. Anorg. Chem.* **1949**, *259*, 278.
(2) Shodai, T.; Okada, S.; Tobishima, S.; Yamaki, J. *Solid State Ionics* **1996**, *86*−*88*, 785.
(3) Nishijima, M.; Kagohashi, T.; Takeda, Y.; Imanishi, M.; Yamamoto, O. *J. Power Sources* **1997**, *68*, 510.
(4) Takeda, Y.; Nishijima, M.; Yamahata, M.; Takeda, K.; Imanishi, N.; Yamamoto, O. *Solid State Ionics* **2000**, *130*, 61.
(5) Rowsell, J. L. C.; Pralong, V.; Nazar, L. F. *J. Am. Chem. Soc.* **2001**, *123*, 8598.
(6) Yang, J.; Wang, K.; Xie, J. *J. Electrochem. Soc.* **2003**, *150*, A140.
(7) Barker, M. G.; Blake, A. J.; Edwards, P. P.; Gregory, D. H.; Hamor, T. A.; Siddons, D. J.; Smith, S. E. *Chem. Commun.* **1999**, 1187.
(8) Gregory, D. H.; O'Meara, P. M.; Gordon, A. G.; Hodges, J. P.; Short, S.; Jorgensen, J. D. *Chem. Mater.* **2002**, *14*, 2063.
(9) Alpen, U. v. *J. Solid State Chem.* **1979**, *29*, 379.
(10) Rabenau, A. *Solid State Ionics* **1982**, *6*, 277.
(11) Gregory, D. H.; O'Meara, P. M.; Gordon, A. G.; Siddons, D. J.; Blake, A. J.; Barker, M. G.; Hamor, T. A.; Edwards P. P. *J. Alloys Compd.* **2001**, *317*−*318*, 237.
(12) Niewa, R.; Huang, Z.-L.; Schnelle, W.; Hu, Z.; Kniep, R. *Z. Anorg. Allg. Chem*. **2003**, *629*, 1778.
(13) The starting material Li_3N was prepared by reaction of molten lithium−sodium alloy with dried nitrogen at 723 K for 4 days.[8,11] Subsequently, excess sodium was removed by vacuum distillation at 723 K. LiNiN was prepared by reaction of Li_3N powder with Ni foil in a N_2 atmosphere at 973−1023 K for 7 days and cooled at ca. 100 K h^{-1}. The Ni foil was pretreated in stream of 20% H_2/80% N_2 at 873 K for 24 h. The resulting gold, lustrous surface layer of crystallites was easily removed from the Ni foil to yield a highly crystalline powder in significant yield (typically ca. 0.5 g).
(14) Powder X-ray diffraction (PXD) data were collected using a Philips XPERT $\theta-2\theta$ diffractometer operating with Cu Kα radiation. The air-sensitive samples were sealed in custom-designed sample holders during data collection. Bulk material was identified as LiNiN by comparison with the PXD pattern generated from single-crystal data[7] using PowderCell 2.3 (Nolze, G.; Kraus W. *Powder Diffr.* **1998**, *13*, 256).
(15) NMR measurements were carried out using a home-built NMR spectrometer based on a Resonance Instruments MARAN DRX pulse programmer and a 4.7 T Oxford Instruments superconducting magnet. Line width measurements were performed using a solid-echo sequence with a $\pi/2$ pulse width of 2.0 μs. T_1 measurements were made using saturation recovery.
(16) Messer, R.; Birli, H.; Differt, K. *J. Phys. C* **1981**, *14*, 2731.
(17) Bertermann, R.; Müller-Warmuth, W. *Z. Naturforsch.* **1998**, *53a*, 863.
(18) Brinkmann, D.; Freudenreich, W.; Roos, J. *Solid State Commun.* **1978**, *28*, 233.
(19) Brinkmann, D.; Mali, M.; Roos, J.; Messer, R.; Birli, H. *Phys. Rev. B* **1982**, *26*, 4810.
(20) Magnetic susceptibility measurements were made using a Quantum Design MPMS XL SQUID susceptometer between 5 and 250 K. Data for LiNiN were fit to a modified Curie−Weiss expression with $\chi_0 = 6.126(6) \times 10^{-3}$ emu mol^{-1}, $C = 0.0158(5)$ emu mol^{-1} K, $\theta = -9.1(5)$ K, and $\mu_{eff} = 0.36$ μ_B per Ni.
(21) Pellets of LiNiN yield resistivity values of 0.16 Ω cm at 293 K. Preliminary DFT results indicate that both $Li_5Ni_3N_3$ and LiNiN are low dimensional metals with E_F located in a partially filled N 2p/Ni 3d π band.
(22) Kerker, G. *Phys. Rev. B* **1981**, *23*, 6312.
(23) Chern, M. Y.; DiSalvo, F. J. *J. Solid State Chem.* **1990**, *88*, 459.
(24) Measured using MAS at 5 kHz between 130 and 473 K.
(25) Gee, B.; Horne, C. R.; Cairns, E. J.; Reimer, J. A. *J. Phys. Chem. B* **1998**, *102*, 10142.
(26) Lee, Y. J.; Wang, F.; Grey, C. P. *J. Am. Chem. Soc.* **1998**, *120*, 12601.

JA039603B